Institut für Veterinärphysiologie
der Vetsuisse-Fakultät Universität Zürich
Direktor: Prof. Dr. Max Gassmann

und

Institut für Molekulare Zellbiologie
Universität des Saarlaandes
Leitung: Prof. Dr. Peter Lipp

Arbeit unter wissenschaftlicher Betreuung von PD Dr. Anna Bogdanova, Vetsuisse-Fakultät Universität Zürich und PD Dr. Lars Kästner, Universität des Saarlandes, Homburg/D

Cardiac remodeling in Gαq and Gα11 knock out mice

Inaugural-Dissertation

zur Erlangung der Doktorwürde der
Vetsuisse-Fakultät Universität Zürich

vorgelegt von

Kathrina Wiesen

Tierärztin
aus Quierschied, Deutschland

genehmigt auf Antrag von

PD Dr. rer. nat. Anna Bogdanova, Referentin 1
PD Dr. rer. nat. Lars Kästner, Referent 2

2015

Institut für Veterinärphysiologie
der Vetsuisse-Fakultät Universität Zürich
Direktor: Prof. Dr. Max Gassmann

und

Institut für Molekulare Zellbiologie
Universität des Saarlaandes
Leitung: Prof. Dr. Peter Lipp

Arbeit unter wissenschaftlicher Betreuung von PD Dr. Anna Bogdanova, Vetsuisse-Fakultät Universität Zürich und PD Dr. Lars Kästner, Universität des Saarlandes, Homburg/D

Cardiac remodeling in Gαq and Gα11 knock out mice

Inaugural-Dissertation

zur Erlangung der Doktorwürde der
Vetsuisse-Fakultät Universität Zürich

vorgelegt von

Kathrina Wiesen

Tierärztin
aus Quierschied, Deutschland

genehmigt auf Antrag von

PD Dr. rer. nat. Anna Bogdanova, Referentin 1
PD Dr. rer. nat. Lars Kästner, Referent 2

2015

Inhaltsverzeichnis **Seite**

Vetsuisse Faculty University of Zürich (2015)

Kathrina Wiesen

Institute of Veterinary Physiology, Vetsuisse Faculty and the Zürich Center for Integrative Human Physiology, University of Zürich, Zürich, Switzerland (sekretariat@vetphys.uzh.ch)

"Cardiac remodeling in Gαq and Gα11 knock out mice"

Abstract

Background

Although both Gαq- and Gα11-protein signaling are believed to be involved in the regulation of cardiac hypertrophy, their detailed contribution to myocardial function remains elusive.

Methods and Results

We studied remodeling processes in healthy transgenic mice with genetically altered Gαq/Gα11-expression, in particular a global Gα11-knockout and a novel inducible cardiac specific Gαq-knockout, as well as a combined double knock-out (dKO) mouse line. Echocardiography revealed that compared with wild type mice, hearts of dKO mice showed an increased ejection fraction and a decreased heart rate, irrespective of age resulting in a maintained cardiac output. We attributed these findings to the lack of Gα11, which absence was associated with a decreased afterload. Histological analysis of the extracellular matrix in the heart depicted a diminished presence of
collagen in aging hearts of dKO mice compared to wild-type mice. The results of a transcriptom analysis on isolated ventricular cardiac myocytes revealed alterations of
the activity of genes involved in the Gαq/Gα11-dependent regulation of the extracellular matrix, such as the matricellular protein Cyr61.

Conclusions

From our data we conclude that Gαq/Gα11 signaling pathways play a pivotal role in maintaining gene activity patterns. For the heart we revealed their importance in modulating the properties of the extracellular matrix, a mechanism that might be an important contributor and mechanistic basis for the development of pressure overload induced cardiac hypertrophy

Keywords

Gαq/Gα11-signalling, cardiac tissue-remodeling, matricellular proteins, Cyr61.

Vetsuisse-Fakultät Universität Zürich (2015)

Kathrina Wiesen

Institut für Veterinär Physiologie, Vetsuisse-Fakultät Universität Zürich und Zentrum für Integrative Human Physiologie, Universität Zürich, Zürich, Switzerland (sekretariat@vetphys.uzh.ch)

"Cardiac remodeling in Gαq and Gα11 knock out mice"

Zusammenfassung

Hintergrund

Obwohl vermutet wird, dass die Signalwege von $G\alpha_q$- und $G\alpha_{11}$-Protein beide in der Regulation von Hypertrophie beteiligt sind, bleibt ihre detaillierte Beteiligung an der myokardialen Funktion unklar.

Methoden und Ergebnisse

Wir haben Umbauprozesse in gesunden transgenen Mäusen mit einer genetisch veränderten $G\alpha_q/G\alpha_{11}$- Signalkette, insbesondere Mauslinien mit einem generellen $G\alpha_{11}$-knockout und einem neuen herzspezifischen $G\alpha_q$-knockout sowie einem kombinierten Doppel knockout (dKO), untersucht. Die Echokardiographie ergab, dass die Herzen der dKO Mäuse im Vergleich zu den Wildtyp Mäusen unabhängig vom Alter ein höheres Auswurfvolumen (EF) und eine niedrigere Herzfrequenz bei gleichbleibendem kardialem Auswurf aufwiesen. Wir führten dies auf die Abwesenheit von $G\alpha_{11}$ zurück, welches mit einer verminderten Nachlast in Zusammenhang gebracht wurde. Histologische Untersuchungen der extrazellulären Matrix im Herzen ergaben ein geringeres Vorkommen von Kollagen in alternden Herzen von dKO Mäusen im Vergleich zu Wildtyp Mäusen. Die Ergebnisse einer Transkriptionsanalyse an isolierten ventrikulären kardialen Myozyten ergaben Veränderungen der Aktivität von Genen, die an der $G\alpha_q/G\alpha_{11}$-abhängigen Regulation der extrazellulären Matrix beteiligt sind, wie das matrizelluläre Protein Cyr61.

Schussfolgerungen

Aus unseren Daten schließen wir, dass $G\alpha_q/G\alpha_{11}$ Signalwege eine Schlüsselrolle in der Aufrechterhaltung von Mustern aktiver Gene spielen. Für das Herz zeigten wir ihre Wichtigkeit bei der Modulation des Grades/ Anteils der extrazellulären Matrix. Dieser Mechanismus sollte einen bedeutenden Beitrag für die Entwicklung einer durch Drucküberlastung induzierten kardialen Hypertrophie leisten und dessen mechanische Basis darstellen.

Stichworte

Gαq/Gα11-Signale, kardialer Gewebeumbau, matrizelluläre Proteine, Cyr61.

International Journal of Cardiology 202 (2016) 836–845

Contents lists available at ScienceDirect

International Journal of Cardiology

journal homepage: www.elsevier.com/locate/ijcard

Cardiac remodeling in $G\alpha_q$ and $G\alpha_{11}$ knockout mice☆,☆☆

Kathrina Wiesen [a,b], Elisabeth Kaiser [b], Laura Schröder [b], Anke Scholz [b], Sandra Ruppenthal [b], Jan-Christian Reil [c], Christina Backes [d], Eckart Meese [d], Carola Meier [e], Anna Bogdanova [a], Peter Lipp [b,*,1], Lars Kaestner [b,*,1]

[a] Institute of Veterinary Physiology, Vetsuisse Faculty and the Zürich Center for Integrative Human Physiology, University of Zürich, 8057 Zürich, Switzerland
[b] Institute for Molecular Cell Biology and Research Centre for Molecular Imaging and Screening, Saarland University, 66421 Homburg/Saar, Germany
[c] Clinic for Internal Medicine III, Saarland University, 66421 Homburg/Saar, Germany
[d] Institute for Human Genetics, Saarland University, 66421 Homburg/Saar, Germany
[e] Anatomy, Saarland University, 66421 Homburg/Saar, Germany

ARTICLE INFO

Article history:
Received 11 July 2015
Received in revised form 29 September 2015
Accepted 3 October 2015
Available online 09 October 2015

Keywords:
$G\alpha_q/G\alpha_{11}$-signaling
Cardiac tissue-remodeling
Matricellular proteins
Cyr61

ABSTRACT

Background: Although both $G\alpha_q$- and $G\alpha_{11}$-protein signaling are believed to be involved in the regulation of cardiac hypertrophy, their detailed contribution to myocardial function remains elusive.
Methods and results: We studied remodeling processes in healthy transgenic mice with genetically altered $G\alpha_q/G\alpha_{11}$-expression, in particular a global $G\alpha_{11}$-knockout and a novel inducible cardiac specific $G\alpha_q$-knockout, as well as a combined double knockout (dKO) mouse line. Echocardiography and telemetric ECG recordings revealed that compared with wild type mice, hearts of dKO mice showed an increased ejection fraction and a decreased heart rate, irrespective of age resulting in a maintained cardiac output. We attributed these findings to the lack of $G\alpha_{11}$, which the absence was associated with a decreased afterload. Histological analysis of the extracellular matrix in the heart depicted a diminished presence of collagen in aging hearts of dKO mice compared to wild-type mice. The results of a transcriptome analysis on isolated ventricular cardiac myocytes revealed alterations of the activity of genes involved in the $G\alpha_q/G\alpha_{11}$-dependent regulation of the extracellular matrix, such as the matricellular protein Cyr61.
Conclusions: From our data we conclude that $G\alpha_q/G\alpha_{11}$ signaling pathways play a pivotal role in maintaining gene activity patterns. For the heart we revealed their importance in modulating the properties of the extracellular matrix, a mechanism that might be an important contributor and mechanistic basis for the development of pressure-overload induced cardiac hypertrophy.

1. Introduction

In the mammalian heart, a plethora of processes are either controlled or modulated via G-protein coupled receptors (GPCRs), which induce intracellular signal transduction [1]. Although the roles of the $G\alpha_i$-, $G\alpha_o$- and $G\alpha_s$-proteins in excitation generation and myocardial function are well understood, the detailed contribution of the $G\alpha_q$- and $G\alpha_{11}$-proteins, as well as their signaling cascades, remain elusive [2–4]. Although the involvement of $G\alpha_q$ in hypertrophic signaling in the heart has been reported [5–8], the detailed signaling processes underlying this phenomenon remain unclear, and the role played by both, physiological responses and homeostasis are not well understood.

Because receptor agonists often trigger multiple signaling pathways simultaneously, dissecting the contributions of both $G\alpha_q$- and $G\alpha_{11}$-protein coupled signaling has proven difficult; cross talk involving β-adrenergic $G\alpha_s$ signaling has been proposed as a mechanism underlying this process [9–11]. Therefore, the transgenic modulation $G\alpha_q$- and $G\alpha_{11}$-protein expression appears to be the method of choice to investigate their involvement in cardiac signaling. Because $G\alpha_q$ and $G\alpha_{11}$ are often regarded as redundant signaling molecules [12], it seems advantageous to knock out both proteins simultaneously.

To characterize basic cardiac functions under physiological conditions, we investigated the hearts of mice in vivo following the induction of the heart specific $G\alpha_q$ knockout, in both, the presence and the absence of $G\alpha_{11}$ proteins. Using such mice, we studied their growth,

☆ All authors take responsibility for all aspects of the reliability and freedom from bias of the data presented and their discussed interpretation.
☆☆ This research was funded by the Clinical Research Unit 196 (DFG [German Research Foundation]), and Saarland University (HOMFOR [Homburger Forschungsförderprogramm] and ZFK [Central Research Commission]).
* Corresponding authors.
E-mail addresses: peter.lipp@uks.eu (P. Lipp), lars_kaestner@me.com (L. Kaestner).
[1] Shared senior authorship.

http://dx.doi.org/10.1016/j.ijcard.2015.10.069
0167-5273/

blood pressure, heart rate variability and life expectancy, and followed both, cardiac morphology and function, via echocardiography over a time period of 9 months. We complemented these in vivo studies with the histological analysis of the extracellular matrix in those hearts and related such findings to a detailed genetic analysis of the myocytes' transcriptome by Next-Generation Sequencing.

2. Materials and methods

2.1. Experimental animals

The experiments were conducted in accordance with the recommendations of the Guide for the Care and Use of Laboratory Animals of the National Institutes of Health. The protocol was approved by the State Office for Health and Consumer Protection (Permit Number: 31/07). All efforts were made to minimize suffering of animals. The transgenic mouse lines were bred using a new Cre-mouse strain, which was recently introduced [13]. For the principle selection of the genotypes of the single knock-out mice and the control animals, we followed previous recommendations [14]. The selection of these genotypes, as well as the abbreviations used in this paper, are summarized in Table 1.

To induce Cre-recombinase activation, a daily dose of Tamoxifen (Sigma-Aldrich, St. Louis, MO, USA) (40 mg/kg body weight) was injected into 5 week-old animals intraperitoneally (i.p.) for 5 days.

The survival times of the mice were compared using PRISM (GraphPad Software, La Jolla, CA, USA), employing the Gehan–Breslow–Wilcoxon Test.

2.2. Imaging of fluorescence protein expression in selected organs and isolated cardiomyocytes

Fluorescence images of the heart, spleen, lung, liver, kidney, aorta, and smooth muscle were obtained using a fluorescence stereomicroscope (SZX12, Olympus, Tokyo, Japan). Ventricular myocytes were isolated according to a protocol established for rat ventricular myocytes [15] with slight modifications, as outlined in [16].

Cellular imaging was performed using a confocal scanner (CSU-10, Yokogawa Corp., Tokyo, Japan) attached to an upright microscope (E600, Nikon, Tokyo, Japan), using a 40× water immersion objective as previously described [17].

2.3. Western blot analysis and control of cardiomyocyte specific Cre-expression

Western blots were performed as previously described [18]. Protein extracts were prepared from freshly isolated cells. The cells were washed 2 times with ice-cold phosphate buffered saline (PBS). Thereafter, ice-cold extraction buffer (in mmol/L: 100, Tris–HCl; 100, NaCl; pH 7.5; 20 DTT, 0.5% Triton-X-100 and a protease inhibitor cocktail: complete, Roche Diagnostics, Mannheim, Germany) was added, and the cells were transferred to a 1.5 mL centrifugation tube. Following a 15 min incubation period on ice to lyse the cells, the lysate was centrifuged at 13.000 *g* in a chilled centrifuge for 15 min. The supernatant was subsequently transferred to a new centrifuge tube, and the protein concentration was determined. The proteins were separated on 10% SDS-PAGE (Bio-Rad, Hercules, CA, USA) according to the Laemmli procedure and electrophoretically transferred to PVDF membranes (GE Healthcare, Chalfont St Giles, UK). The membranes were blocked using 5% skim milk in PBS plus 0.1% v/v Tween-20 before incubation with mouse anti-α-tubulin antibody, 1:1000 (Sigma-Aldrich, St. Louis, MO, USA), and rabbit anti-$G\alpha_q$ antibody, 1:1000 (Santa Cruz Biotechnology, Dallas, TX, USA). HRP-conjugated secondary antibodies, 1:30000 (Santa Cruz Biotechnology, Dallas, TX, USA), and an ECL plus Western Blotting detection system (GE Healthcare, Chalfont St Giles, UK) were used to detect the proteins of interest.

2.4. Blood pressure measurements

Blood pressure was monitored online in mice with implanted telemetric pressure sensors with the catheter placed directly into the aortic arch (HD-X11, Data Sciences International, St. Paul, MN, USA).

Table 1
Overview of the mouse genotypes used with explanations of the expression of the modified proteins; wt = wild-type; tg = transgenic (Cre expression); 0 = no Cre expression. The lines' background color corresponds to the color-code used throughout all figures.

Label	gnaq	gna11	Cre status	Tamoxifen	Abbreviation
$Gq^{fl}G11^{wt}Cre^{-}Tam^{+}$	flox/flox	wt/wt	0/0	+	WT
$Gq^{fl}G11^{wt}Cre^{+}Tam^{+}$	flox/flox	wt/wt	tg/0	+	Gq-KO
$Gq^{fl}G11^{-}Cre^{-}Tam^{+}$	flox/flox	-/-	0/0	+	G11-KO
$Gq^{fl}G11^{-}Cre^{+}Tam^{+}$	flox/flox	-/-	tg/0	+	dKO

Thirty-two-week-old male mice were anesthetized (3% Isoflurane for induction, 1.5% for maintenance, analgesia: Carprofen (10 mg/kg body weight) prior to being placed in the dorsal recumbent position on a heating plate. The animals' forelimbs were taped to the table following a lack of an observed response to the paw pinch test. A midline incision through the skin from the mandible to the sternum enabled clinicians to view the underlying salivary glands. The glands were gently separated, and the left carotid artery was carefully isolated from the surrounding using blunted, curved forceps. Three 10 cm pieces of suture (silk, 6/0, Suprama, Berlin, Germany) were positioned under the artery. The most distal cranial suture was tightly ligated at the height of the bifurcation of the internal and external carotid arteries. A loose knot at the two other ligatures and an additional microserrefine suture temporarily occluded blood flow to prevent bleeding during cannulation and pressure catheter insertion. The carotid artery was pierced using a modified 26-gauge needle proximal to the permanent knot, and the artificial hole was held in place with this needle as the tip of the pressure catheter was inserted. With the help of vessel cannulation forceps, the catheter was advanced until the tip reached the aortic arch. The serrefine suture was subsequently removed, and the loose ligatures were released to allow passage of the catheter before being tightened again to keep the catheter in position after it reached the aortic arch. The systemic pressure was immediately recorded (Dataquest A.R.T, Data Sciences International, St. Paul, MN, USA) and sampled over a two minute period (sampling rate: 500 Hz). The animals were decapitated immediately following the withdrawal of the catheter.

The Gaussian distribution of the mean arterial pressure values was verified using the Kolmogorov–Smirnov test. Comparisons of significance were performed with an unpaired t-test.

2.5. Echocardiography

Echocardiography was performed with a device designed for small animals (Vevo 770, Visualsonics, Toronto, Canada). For a minimum of 1 h, the mice were placed under a warming lamp in the room in which echocardiography was performed to acclimatize them to their surroundings. For echocardiography, the mice were anesthetized in an induction chamber with a constant inflow of 3% isoflurane mixed with pure oxygen. When they stopped exhibiting positional reflexes, they were removed from the chamber and placed on a heated platform with embedded ECG contact pads in the dorsal recumbent position; 1–2% isoflurane mixed with pure oxygen flow was administered via facemasks. The eyes were covered with dexpanthenol (Bepanthen, Bayer, Wuppertal, Germany) eye ointment to avoid dehydration, and the paws were taped to the ECG contact pads. To maintain body temperatures above 36 °C, a warming lamp was positioned above the mice, and temperature was monitored via a rectal probe. The hair on the ventral side of the thorax was removed with hair removal solution (Nair hair removal, Church & Dwight, Ewing, NJ, USA). Ultrasound gel was warmed to 37 °C and placed on the chest, primarily in the area above the heart, before the 30 MHz scan head was utilized.

We performed B- and M-mode imaging in both long and short axis views to measure interventricular septum thickness (IVS), left ventricular inner diameter (LVID), and left ventricular posterior and anterior wall thickness (LVPW and LVAW) during both systole and diastole. The Vevo 770 program calculated left ventricular (LV) mass, LV systolic and diastolic volume, ejection fraction (EF) and fractional shortening (FS). To image the trans-mitral flow pattern, the probe was positioned orthogonally relative to the apex of the heart, in the left ventricle, at the tip of the mitral valve. In Pulse-waved Doppler (PWD) mode, mitral valve (MV) velocity (MVE = Early diastolic filling wave; MVA = Atrial kick wave) and isovolumic relaxation time (IVRT) were both measured.

Lines connecting different time points do not impose a functional dependence but were drawn as guides for the eye.

In the control experiments, the Adenosine A_1 receptor ligand 2-Chloro-N^6-cyclopentyladenosine (CCPA; Sigma-Aldrich, St. Louis, MO, USA) was administered to decrease the animals' heart rates without triggering additional signaling pathways in the myocardium.

For the statistical analysis of the echocardiographic parameters, we performed a 2-way ANOVA test in PRISM (GraphPad Software, La Jolla, CA, USA) to examine the differences between the genotypes.

2.6. Heart rate variability

For Heart rate variability (HRV) analysis, biopotential transmitters were implanted as described above (Section 2.4 Blood pressure measurements). To enable ECG recordings, the positive lead was fixed subcutaneously 10 mm left to the manubrium sterni, the negative lead on the right pectoral muscle. The mice were allowed the recover for at least 2 weeks and kept in a light/dark schedule of 12/12 h. In 20 week old mice of all genotypes, ECGs were acquired for a 60 h period with hourly measurements of 5 min duration (Dataquest A.R.T, Data Sciences International, St. Paul, MN, USA). For HRV analysis, we selected 18–23 segments of 2 min from 13 animals during light periods, which were free of artifacts and ectopic beats. Analysis was performed according to the recommendations by Thireau et al. [19]. We calculated the mean normal-R to normal-R intervals (NN) and the standard deviation of NN intervals (SDNN). Further parameters are presented in [20]. All calculations were performed with Labchart and Labchart Pro (AD Instruments, Unit B, Bishops Mews, Transport Way, Oxford OX4 6HD, UK). Statistical analysis was executed in PRISM (GraphPad Software, La Jolla, CA, USA). The Gaussian distribution was checked using the D'Agostino & Pearson omnibus normality test. Comparison of significance was performed with an unpaired t-test for Gaussian distributed data (plotted

as bar graphs) or with a Mann–Whitney test for non-Gaussian distributed data (plotted as boxes).

2.7. Cardiac function

The hearts were examined using a procedure similar to that previously described [21]; the mice were heparinized with 100 IU heparin 15 min prior to being killed via the intraperitoneal administration of pentobarbital-sodium (60 mg/kg body weight). The heart was excised and placed in ice-cold St. Thomas-Hospital solution (Dr. Franz Köhler Chemie GmbH, Bensheim, Germany). Following removal of the pericardium, lungs, and trachea, the aorta was cannulated using an 18-gauge metal cannula. The left atrium (LA) was also cannulated through the pulmonary vein using a 1.5 cm, 16-gauge steel cannula. This cannula was connected to a heated preload column, resulting in a myocardial temperature of 37 °C when the heart was working (preload 10 mm Hg, afterload 60 mm Hg). The hearts were paced at the RA at 380 beats per minute. Left ventricular (LV) systolic and diastolic function were both recorded using a conductance catheter (Millar 1.4F SPR-835, Millar, Houston, TX, USA) inserted into the LV cavity through a small hole in the apex. The LV pressure–volume relationship [end-systolic pressure–volume relationship (ESPVR) and end-diastolic pressure—volume relationship (EDPVR)] were investigated under following a sudden increase in the afterload from 80 mm Hg to 120 mm Hg(EDPVR), resulting in beat-to-beat changes as the heart slowly adjusted to the increased afterload. Both the cardiac inflow (1/4 cardiac output, CO) and aortic flow were recorded continuously using inline ultrasonic transit probes and were subsequently used to calibrate volume measurements, using a conductance catheter. Parallel conductance (wall thickness) was determined using the saline dilution method, which involved injecting a 5 mL bolus of hypertonic (5%) saline into the left atrial cannula, causing a transient change in the conductivity of KHB in the LV.

2.8. Histology

The mice were anesthetized via the intraperitoneal injection of pentobarbital-sodium (60 mg/kg body weight) and subsequently killed via decapitation. Following a midline sternal incision, the hearts were quickly excised and washed in freshly provided 4% paraformaldehyde (PFA) in phosphate buffered saline, pH 7.4, to remove the blood from the ventricles. They were then placed in 2 mL Eppendorf tubes filled with 4% PFA and stored in a fridge at 4 °C until needed. The hearts were dehydrated using an ascending ethanol series before being embedded in paraffin wax, and then sectioned into 6 μm thick slices with the help of a microtome (HM350, Microm, Heidelberg, Germany).

For staining, the slices were rinsed 3 times in xylol and decreasing isopropanol concentrations before being washed in aqua dest. and subjected to pico-Sirius Red staining solution. After 1 h, the staining solution was differentiated in HCl and increasing isopropanol concentrations.

Images of the stained slices were taken on a NIKON E600 upright microscope equipped with a DS-Ri1 Camera (Nikon, Tokyo, Japan), and subsequently analyzed using LUCIA F/G. The measurements were performed on 10 images from different parts of the left ventricle.

Significance of 8 week old vs. 50 week old mice was tested using Sidak's multiple comparison test and the comparison of the different genotypes at particular time points was performed with the Mann–Whitney test using PRISM (GraphPad Software, La Jolla, CA, USA).

2.9. Next-Generation Sequencing

To investigate changes of the transcriptome, adult ventricular myocytes from three WT and three dKO animals were investigated via Next Generation Sequencing, using HiSeq 2000 (Illumina, San Diego, CA, USA) with 60 million reads per library. For a cardiomyocyte specific RNA extraction total RNA was extracted from isolated cardiac myocytes to obtain. Cell isolation was modified from a protocol originally established for the isolation of rat cardiac myocytes [15]. Animals were anesthetized (10 mL/kg body weight) i.p. with a mixture of ketamine hydrochloride (85 mg/kg body weight) and xylazine hydrochloride (15 mg/kg body weight) dissolved in 0.9% NaCl solution. Anesthesia was considered sufficient when the paw pinch test was negative. We subsequently injected citrate (117 mg/kg body weight) i.p. to reduce blood clotting. The animals were killed via decapitation. Solution A^+ (in mmol/L: NaCl, 134; KCl, 4; glucose, 11; $MgSO_4$, 1.2; Na_2HPO_4, 1.2; HEPES, 10; EGTA, 0.2; pH adjusted to 7.35 using NaOH) was injected into both ventricles to arrest the heart and remove blood. The hearts were then cannulated to allow retrograde Langendorff perfusion with solution A^+ at room temperature for 5 min. Following Liberase (Roche Diagnostics, Mannheim, Germany) perfusion (1 mg in solution A) at 37 °C for 12 min, the hearts were placed in petri dishes with solution A (in mmol/L: NaCl, 134; KCl, 4; glucose, 11; $MgSO_4$, 1.2; Na_2HPO_4, 1.2; HEPES, 10; pH adjusted to 7.35 using NaOH and sterile filtered, oxygenated saline). The ventricles were cut and triturated and paced in solution A plus DNAse I Type 2 (Sigma-Aldrich, St. Louis, MO, USA; 4 units per mL) for 10 min. The cells were seeded in 10 cm petri dishes coated with extracellular matrix proteins (Sigma-Aldrich, St. Louis, MO, USA). Following a sedimentation period of 30 min at 37 °C, the cells were rinsed with PBS and harvested. RNA extracts were prepared using an RNeasy Mini Kit (Qiagen, Hilden, Germany) according to the manufacturer's instructions. RNA concentrations were measured using NanoDrop (ThermoScientific, Wilmington, DE, USA), and quality control was performed using an Agilent 2100 bioanalyzer (Agilent Technologies, Böblingen, Germany). cDNA library construction and sequencing were each performed using GATC Biotech AG (Konstanz, Germany).

The generated RNA-seq data were mapped against the NCBI mouse reference genome (build37.2) using TopHat 2.0.9 [22]. We subsequently used the Cufflinks package to identify differentially expressed genes [23]. We followed the protocol for mapping and identifying differentially expressed genes developed by Trapnell et al. [24]. We removed the differentially expressed genes having no official name from the resulting list. To identify the regulatory or metabolic pathways and functional categories that were significantly enriched by the identified genes, we performed an Over-Representation Analysis (ORA) with GeneTrail [25], using both the pathway information from KEGG [26] and the ontologies from GO [27]. Additionally, we performed a Gene Set Enrichment Analysis (GSEA) with GeneTrail by sorting the full gene list by their fold changes in such a way that the genes over-expressed in the dKO group were at the top of the list. As both enrichment analyses yielded many significant categories, we considered only those that were significant in both the ORA and the GSEA analyses.

3. Results

3.1. The inducible cardiomyocyte specific knock-out of $G\alpha_q$

We aimed to generate a mouse model in which the $G\alpha_q$ gene was inactivated in both a tissue-specific and an inducible manner. Using transgenic mouse lines ($G\alpha_{11}^{-/-}$ and $G\alpha_q^{flox/flox}$) [8], we created a novel cardiac specific inducible knock-out for $G\alpha_q$, utilizing a recently introduced α-MHC-CreER(T2) mouse line [13]. We refer to these mice as $Cre^{tg/0}$ instead of α-MHC-CreER(T2). Because the $Cre^{tg/0}$ mouse line has not been characterized before, we crossed it with the mT/mG reporter mouse line [28] to obtain mT/mGtg/0 Cretg/0 offspring and investigated tissue specificity of expression. Cre recombinase activity was induced via Tamoxifen (see Materials and methods), and miglyol injection was used as a negative control. Fig. 1 depicts that tissue-specific $G\alpha_q$ down regulation was achieved 21 days after Tamoxifen injection, as studied by Western blot analysis. Three weeks following the first injection, the hearts of mT/mGtg/0 Cretg/0 offsprings were excised and investigated. While the hearts of miglyol-treated mice exhibited control tdTomato (red) fluorescence (Fig. 1Aa) lacking eGFP (green) fluorescence (Fig. 1Ab), Tamoxifen injections induced an almost complete loss of the red fluorescence from cardiac muscle tissue (Fig. 1Ad) and a strong eGFP fluorescence (green, Fig. 1Ae). To confirm the expected plasma membrane restricted eGFP expression, cardiac tissue was subjected to confocal imaging (Fig. 1E). Our results clearly depicted the presence of eGFP in the plasma membrane. Fig. 1D further details the tissue-specificity of the $Cre^{tg/0}$ mouse. Using fluorescence microscopy, only the heart tissue exhibited a high $F_{eGFP}/F_{tdTomato}$ ratio while all other tissues displayed ratios that were at least 6–10 fold smaller (Fig. 1D).

Additionally, we scrutinized this Cre approach in $G\alpha_{q/11}$ double-knock-out (dKO) mice ($Gq^{fl}G11^{-}Cre^{+}Tam^{+}$) to characterize both the degree and the speed of $G\alpha_q$ loss. The expression of $G\alpha_q$ in isolated ventricular myocytes was probed by Western blots at various times after Tamoxifen administration (Fig. 1B). The signals approached the detection level at 23 days after injection. Fig. 1C summarizes results of a series of experiments including comparisons of the time dependent loss of $G\alpha_q$ proteins (filled symbols) and the change in eGFP/tdTomato fluorescence ratio (open symbols).

These results confirmed both the functionality of the heart specific inducible Cre/loxP system and the almost complete loss of $G\alpha_q$ expression in ventricular myocytes three weeks after the first Tamoxifen injection.

3.2. Basic characterization in vivo

Fig. 2 summarizes the results of a basic longterm study investigating the various genotypes. We found no differences in the growth of the mice (Fig. 2A). However, as depicted by the Kaplan–Meyer survival curves of the four genotypes in Fig. 2B, the lifespan of the dKO was significantly increased compared with both the Gq-KO and the WT mice. Although the lifespans of the Gq-KO and the G11-KO mice were

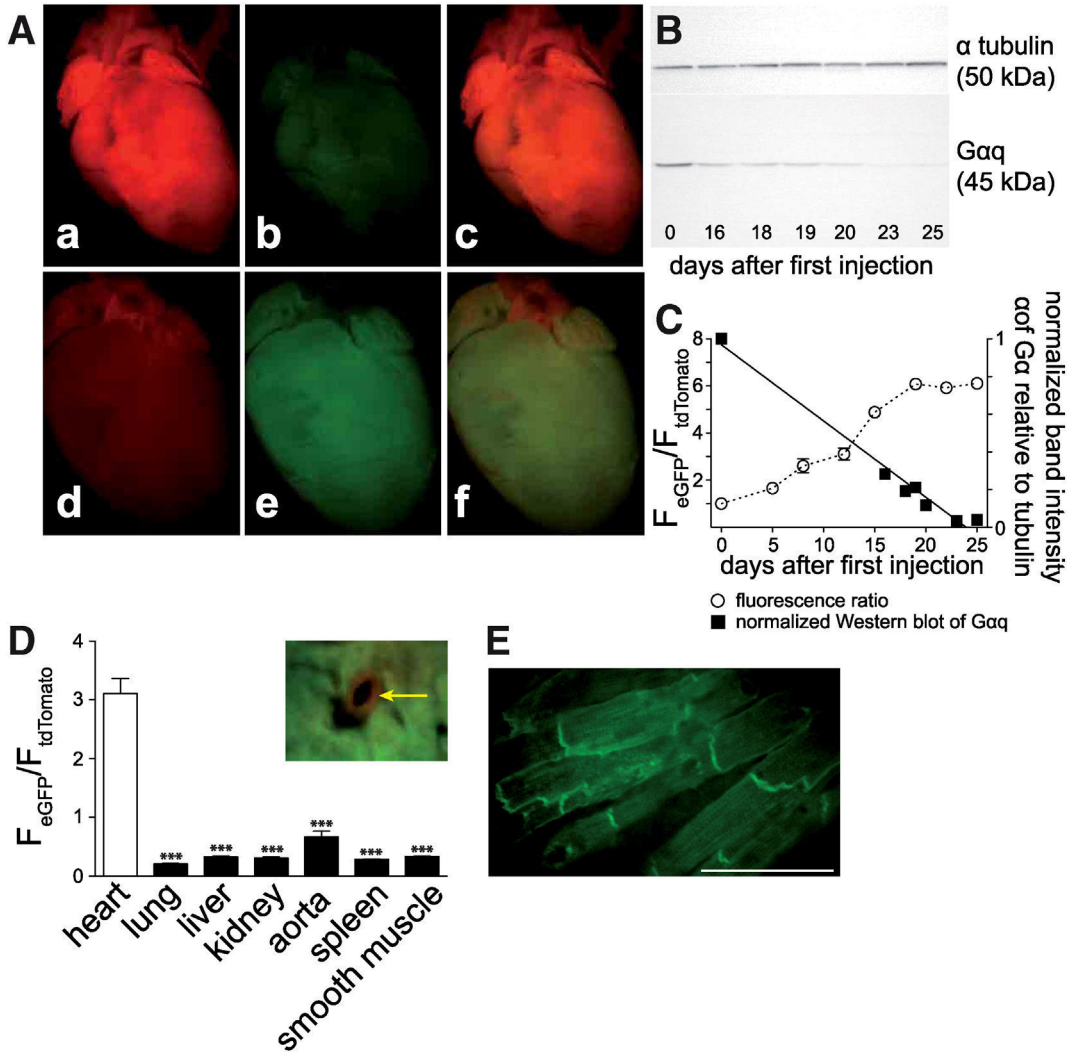

Fig. 1. Tissue specificity and time course of the Cre-induced down-regulation of Gαq following Tamoxifen injection. (A) Depicts hearts from double fluorescent Cre reporter mice (for details see Materials and methods). The heart in (a)–(c) has been injected with miglyol while the heart in (d)–(f) has been Tamoxifen-injected (22 days after the start of the first Tamoxifen injection). The first column (a) & (d) depicts the red fluorescence (tdTomato), the second column (b) & (e) the green fluorescence (eGFP). All four images are recorded under identical conditions. Sub-panels (c) & (f) show overlays of images (a) & (b) and (d) & (e), respectively. (B) shows a typical Western blot from isolated ventricular myocytes in which we probed for Gαq with α-tubulin as the loading control. The times after first Tamoxifen injection are given below. (C) summarizes the data from (A) and (B). (D) displays a statistical summary of the green/red fluorescence ratio from images such as those shown in (A) for various tissues. Tissues were sampled at day 12 after the first Tamoxifen injection and were taken from 12–27 animals. Inset: view onto a cut open heart depicts cardiomyocyte specific eGFP expression (green) and non-cardiomyocyte-specific tdTomato expression in coronary vessels (red, marked with a yellow arrow). (E) confocal image of cardiac tissue highlighting the membrane targeted eGFP. The outline of individual cardiomyocytes 12 days following Tamoxifen injection can be discerned. The white scale bar represents 100 μm. (For interpretation of the references to color in this figure legend, the reader is referred to the web version of this article.)

not significantly different, their p-value of 0.056 was close to the defined significance level. We investigated the cause of death post-mortem and found that the majority of mice died because of infirmity. Nevertheless, we observed the presence of tumors in 25% of the animals but were unable to observe a significant prevalence in a particular genotype (data not shown).

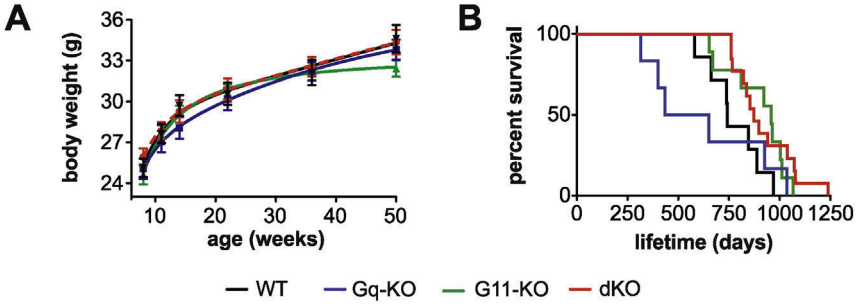

Fig. 2. Growth and lifetime of WT, G11-KO, Gq-KO and dKO mice. (A) shows a summary of the growth of all genotypes tested starting from the age of 8 weeks ($G\alpha_q$-protein downregulated) up to the age of 50 weeks. There was no statistical difference in the growth of all mice investigated. (B) Kaplan Meier survival plot for all genotypes. A statistical comparison of the survival curves yielded: dKO vs. WT, $p = 0.034$ (*); dKO vs. Gq-KO, $p = 0.029$ (*); G11-KO vs. WT, $p = 0.12$ (n.s.); G11-KO vs. Gq-KO, $p = 0.056$ (n.s.); Gq vs. WT, $p = 0.31$ (n.s.); and dKO vs. G11, $p = 0.92$ (n.s.).

The same population of animals as in Fig. 2 were subjected to repetitive echocardiography to characterize basic cardiac parameters in vivo [18]. The animals were examined at the age of 8 weeks (3 weeks after Tamoxifen injection), 11, 14, 22, 36 and 50 weeks.

Left ventricular inner diameter (LV ID), left ventricular posterior wall thickness (LV PW), left ventricular anterior wall thickness (LV AW) and inner ventricular septum thickness (IVS) were not significantly different among the different genotypes (see Fig. 1 in [20]) indicating no alteration in normal heart development.

Interestingly, in contrast to such morphometric parameters, the hearts of the dKO mice exhibited significantly increased ejection fractions (EF, Fig. 3Ba) and fractional shortening (FS, see Fig. 2 in [20]) when compared with the WT mice. See also the exemplified M-mode images in Fig. 3Ab. Additionally, the mitral valve E/A-wave ratio was significantly increased in the dKO mice when compared with the WT mice (see Fig. 2 in [20]). Noteworthy, the particular analysis of the two single KO mouse lines yielded values for these functional parameters in between those for WT and dKO (see Fig. 2 in [20]). We detected

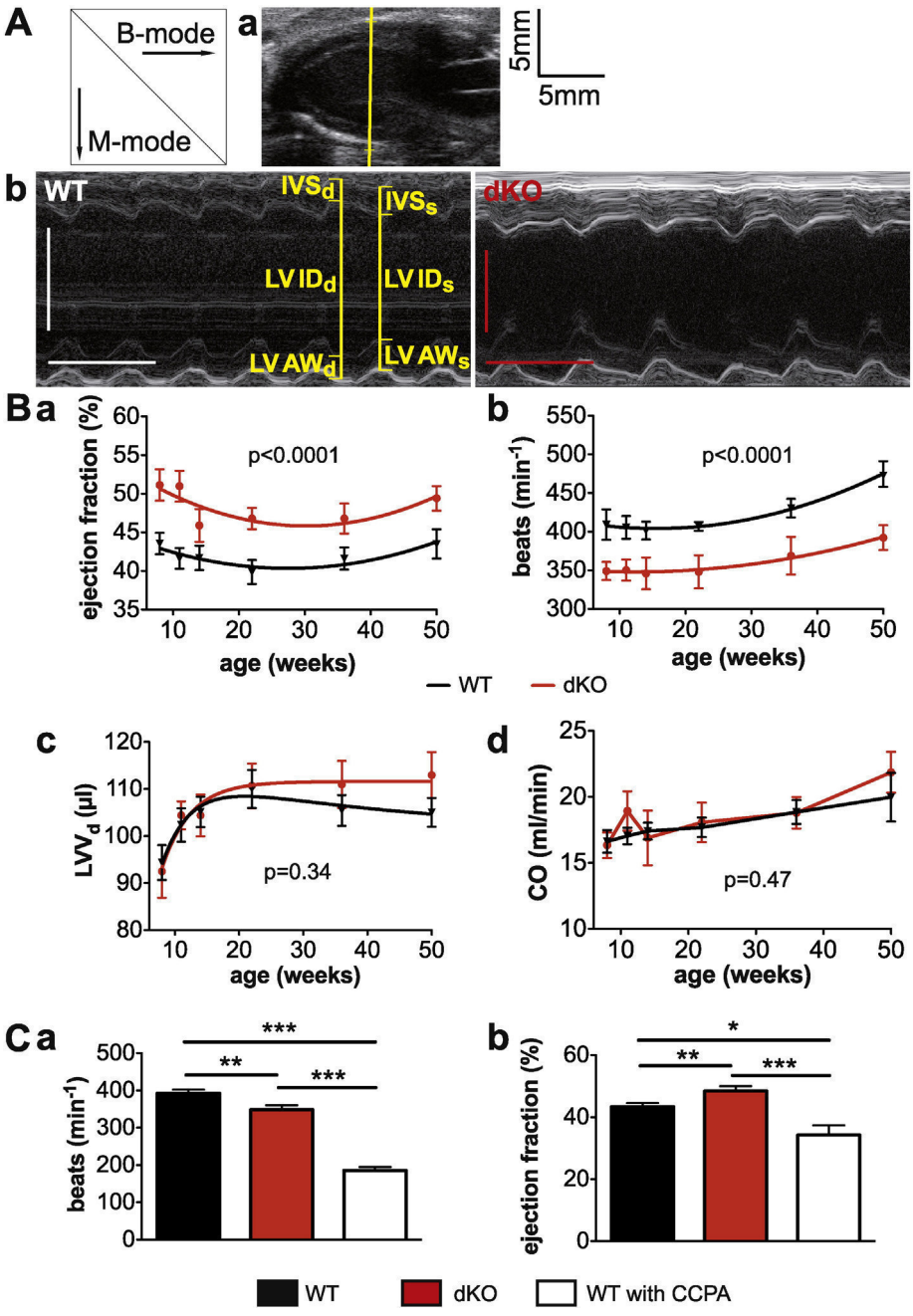

Fig. 3. Functional analysis of WT and dKO mice. (Aa) Echocardiographic B-mode image for a WT mouse with the yellow line indicating the position for the M-mode images. (Ab) Representative M-mode images of a WT mouse heart (left) and a dKO mouse heart (right) at the age of 50 weeks. The horizontal scale bars depict 200 ms and the vertical scale bar 3 mm. In yellow a selection of morphometric parameters that can be deduced from the M-mode image are highlighted. (B) Development of EF (Ba), heart rate (Bb), left ventricular diastolic volume (LVV_d, Bc) and cardiac output (CO, Bd) over time for WT (black) and dKO mice (red). All data derived from 12–16 animals per group. The full set of morphometric and functional parameters for all four genotypes is summarized in Figs. 1 & 2 in [20]. (C) A decreased heart rate is associated with a decreased ejection fraction in WT (black and white bars) but not in dKO mice (red). In WT the heart rate was substantially decreased by the administration of the negative chronotropic agent CCPA. Each bar summarizes the results from 9–11 animals. (For interpretation of the references to color in this figure legend, the reader is referred to the web version of this article.)

a significantly slower heart rate in the dKO mice in comparison to WT for all age groups (Fig. 3Bb). Such changes were not based on changes in the hearts volume (Fig. 3Bc) nor in the cardiac output, CO (Fig. 3Bd). To investigate whether the slower rate was compensatory for the larger EF and FS we measured the ejection fraction in WT, dKO and WT treated with CCPA. CCPA is an adenosine receptor A_1 agonist, which decreases the conduction of electrical impulses and suppresses pacemaker cell function, resulting in a decrease in heart rate [29]. Fig. 3C summarizes the results of such a study. Although CCPA treated WT animals displayed a substantially reduced heart rate, EF was not increased as in the dKO but instead decreased (see Fig. 3Cb).

3.3. Mechanism of altered contractility

We subsequently evaluated cardiac performance under well-defined ex vivo conditions independent of either systemic influences or acute hormonal modulations by measuring functional parameters in explanted working hearts as described in Materials and methods. Fig. 4A summarizes such functional measurements. Representative

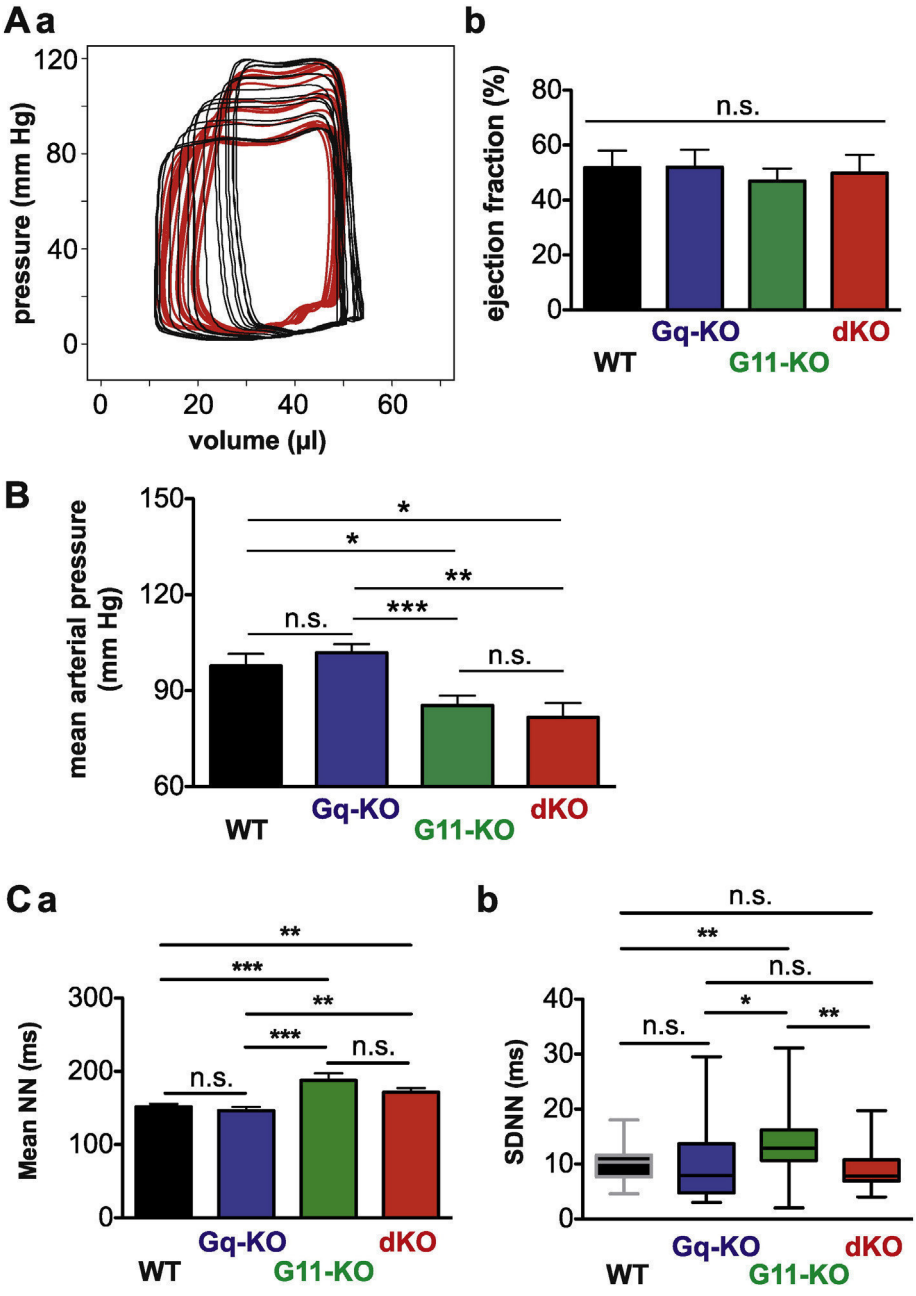

Fig. 4. Ejection fraction in the isolated working heart and mean arterial pressure and heart rate variability in vivo. (Aa) Representative examples of pressure–volume loops measured in ex vivo working hearts from 32 week old WT (black) and dKO (red) mice. (Ab) Statistical analysis of the ejection fraction of working hearts obtained from mice of given genotypes. Each bar comprises the results of 5–10 mice. (B) Mean arterial pressure measured in vivo in 32 week old mice. Mice with a global G11-KO displayed a reduced mean arterial pressure (9–12 animals per genotype). (C) Heart rate variability (HRV) analysis based on telemetric ECG measurements in conscious freely moving 20 week old mice. (Ca) Mean R–R intervals (Mean NN) and (Cb) standard deviation of all normal R–R intervals (SDNN). Diagrams represent measurements from 13 mice. (For interpretation of the references to color in this figure legend, the reader is referred to the web version of this article.)

pressure–volume loops for both hearts from WT and dKO mice are depicted in Fig. 4Aa, while Fig. 4Ab displays the ejection fraction calculated from working heart experiments for each genotype. Interestingly, we could not find any significant differences. Additional parameters derived from the working heart study are presented in Fig. 3 in [20].

We thus wondered whether the differences we recorded in vivo were a result of e.g. altered afterload because it has been described that $G\alpha_{11}$-signaling impacts on smooth muscle contractility and might thus influence the mean arterial pressure [30]. We therefore investigated the mean arterial pressure in in vivo telemetric measurements whose results are summarized in Fig. 4B. Noteworthy, the mean arterial pressure was significantly reduced in those genotypes in which G11 was knocked out, i.e. in G11-KO and dKO mice, while Gq-KO animals were not different from WT.

Furthermore, we investigated the heart rate variability (HRV) in freely moving mice (Fig. 4C). First of all we could confirm the decrease of the heart rate in dKO mice initially determined under isoflurane narcosis (Fig. 3Bb). Additionally we could, in similarity to the mean arterial pressure, link the decrease in heart rate to the genotypes with the $G\alpha_{11}$ knockout (Fig. 4Ca). The standard deviation of normal R–R intervals (Fig. 4Cb), representing total autonomic variability gave a significant increase for G11-KO mice compared to all other genotypes. Further time-domain and frequency domain parameters of the HRV depicted no differences between WT and dKO mice (see Fig. 4 in [20]).

3.4. Histology for collagen

Based on previous reports that following transaortic constriction (TAC) mice lacking $G\alpha_q$ and $G\alpha_{11}$ failed to develop hypertrophy [8], we speculated as to whether collagen production was altered in vivo when modulating such signaling pathways. Apart from pathological alterations of the collagen content, it is well established that the proportion of collagen in the heart is increasing with progressing age. We thus wondered whether increased fibrosis accompanying physiological aging might be affected by $G\alpha_q/G\alpha_{11}$ signaling. To address this, we probed histological sections for collagen content by Sirius Red staining with hearts at three different ages (8-, 22- and 50-weeks) for all four genotypes. Fig. 5A depicts representative sections for all conditions probed, while Fig. 5B summarizes the statistics for a population of mice. Interestingly, WT hearts developed the expected increase in

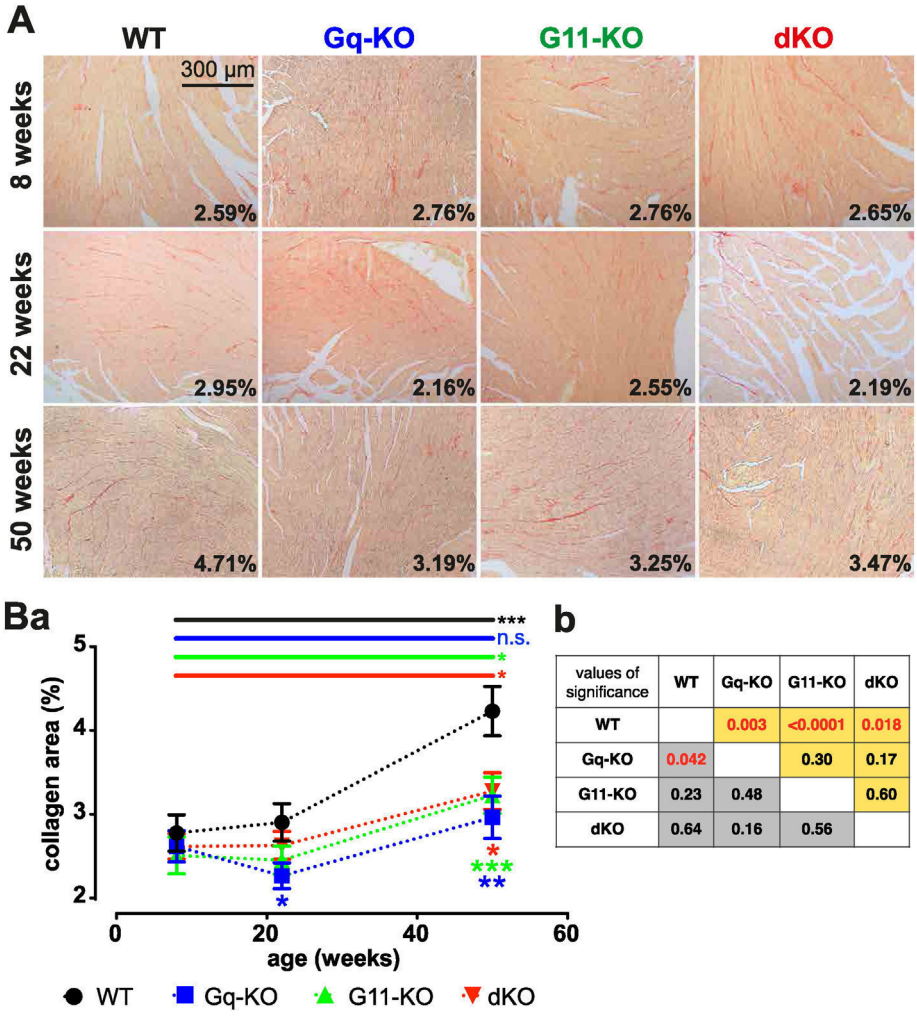

b

values of significance	WT	Gq-KO	G11-KO	dKO
WT		0.003	<0.0001	0.018
Gq-KO	0.042		0.30	0.17
G11-KO	0.23	0.48		0.60
dKO	0.64	0.16	0.56	

Fig. 5. Assessment of fibrosis in aging WT, Gq-KO, G11-KO and dKO mouse hearts. (A) Representative histological sections through hearts of WT, Gq-KO, G11-KO and dKO mice (from left to right) at three different time points (8,22 and 50 weeks, top-down) in which the collagen content was probed by Sirius Red staining. The value in each image gives the fraction of Sirius Red stained area of the entire heart's area. (Ba) Statistical analysis of 30 slices from at least three mouse hearts for each genotype and time point. The bars on top display the statistical analysis of the 8 week vs. 50 week values within each genotype. The bar's color identifies the genotype. Stars below the traces depict statistically significant differences at the given time point for the genotype indicated by the corresponding color against WT. (Bb) Detailed p-value table for the comparisons of all genotypes at the age of 22 weeks (gray cells) and 50 weeks (yellow cells). Black numbers did not reach the significance level of 0.05. (For interpretation of the references to color in this figure legend, the reader is referred to the web version of this article.)

Table 2
Summary of the Next Generation Sequencing analysis of the transcriptome obtained from isolated myocytes of WT and dKO hearts. Only genes coding for major extracellular matrix proteins and matricellular proteins whose transcriptional activity was significantly changed are listed.

Gen group	Gen	Full name	Subtype	Reads WT	Reads dKO	Ratio KO/WT	log2 (fold change)	p-Value
Major extracellular matrix proteins	Col1a1	Collagens	Type 1, α1	21.89	29.31	1.34	0.42	0.0002
	Col1a2		Type 1, α2	25.83	34.16	1.32	0.40	0.0003
	Col3a1		Type 3, α1	35.34	55.19	1.56	0.64	0.0001
	Col4a1		Type 4, α1	75.74	102.2	1.35	0.43	0.0002
	Col4a4		Type 4, α4	0.4925	0.7639	1.55	0.63	0.0001
	Col5a2		Type 5, α2	4.366	5.535	1.27	0.34	0.0046
	Col5a3		Type 5, α3	7.081	9.541	1.35	0.43	0.0003
	Col6a1		Type 6, α1	24.43	35.99	1.47	0.56	0.0001
	Col6a2		Type 6, α2	26.17	37.70	1.44	0.53	0.0001
	Fn1	Fibronectin 1		4.286	8.535	1.99	0.99	0.0001
	Lama2	Laminins	α2	18.36	23.31	1.27	0.34	0.0046
	Lama4		α4	16.94	22.97	1.36	0.44	0.0001
	Lama5		α5	14.62	7.708	0.53	−0.92	0.0001
	Lamb3		β3	4.822	6.337	1.31	0.39	0.0020
	Lamc2		γ2	1.805	1.248	0.69	−0.53	0.0004
	Vtn	Vitronectin		15.24	24.31	1.60	0.67	0.0001
Matricellular proteins	Cyr61	Cysteine-rich angiogenic protein 61	CCN-1	432.8	259.0	0.60	−0.74	0.00005
	Ctgf	Connective tissue growth factor	CCN-2	159.9	129.0	0.81	−0.31	0.0075
	Wisp1	WNT1 inducible signaling	CCN-4	0.5582	0.2094	2.67	−1.41	0.00005
	Wisp2	pathway protein	CCN-5	1.427	2.684	1.88	0.91	0.00005
	Fbln2	Fibulins	Isoform 2	22.67	29.37	1.30	0.37	0.0014
	Fbln5		Isoform 5	4.53	6.15	1.36	0.44	0.0002
	Postn	Periostin		6.127	10.46	1.71	0.77	0.00005
	Sparc	Osteonectin		172.4	250.6	1.45	0.54	0.00005
	Thbs1	Thrombo-spondins	TSP-1	1.201	2.871	2.39	1.26	0.00005
	Comp		TSP-5	0.6756	1.344	1.99	0.99	0.0001

collagen content (black) but the Gq-KO, the G11-KO and the dKO mice depicted a significant lower fibrosis compared to WT mice at 50 weeks of age.

3.5. Molecular analysis

Based on our finding that physiological aging-related fibrosis of the heart was substantially reduced or even absent, we thought of performing a whole transcriptome comparison of cardiac myocytes from WT and dKO-mice to identify possible candidate genes. In the analysis we particular concentrated on collagen and extracellular matrix related gene families as depicted in Table 2. Interestingly, we found that although the mRNA for most collagens was upregulated in myocytes from dKO hearts, members of the large family of matricellular proteins that are known to dynamically regulate the structure and function of the extracellular matrix [31] were significantly downregulated. We found that in particular the mRNA of the highly abundant matricellular protein of the CCN family, Cyr61, was substantially downregulated and would suggest that changes in its expression might play a significant role in our findings.

4. Discussion

In this manuscript we report a novel link between $G\alpha_q/G\alpha_{11}$ signaling and structural remodeling of the heart that might be important during cardiac hypertrophy. Employing a cardiac-specific, conditional Gq-KO mouse strain we were able to downregulate $G\alpha_q$ protein levels in the heart to below detection limits within 3 weeks. In vivo characterization depicted longer lifetimes and substantially lower heart rates with an improved ejection fraction of the dKO mice. In Gq-KO and dKO mice age-dependent increases in fibrosis were absent or substantially decreased, most likely through down regulation of matricellular genes such as for Cyr61 that regulate extracellular matrix formation and signaling.

4.1. Functional characterization of $G\alpha_q/G\alpha_{11}$-KO mouse strains

Understanding the role of $G\alpha_q$-dependent intracellular signaling in the heart requires the availability of tissue-specific inhibitors, activators or tissue-specific KO of the $G\alpha_q$ gene. Here, we introduce a novel cardiac-specific Gq-KO mouse line and its characteristics. In comparison to an earlier Gq-KO mouse line with a non-inducible Cre [8], the mouse line used here was Tamoxifen-inducible, $G\alpha_q$ proteins were downregulated to below detection levels within 3 weeks after Tamoxifen induction and the KO was cardiac-specific as demonstrated by the use of a reporter mouse (Fig. 1).

A thorough in vivo investigation of the cardiac morphology and function gained little differences between the various genotypes used. Nevertheless, dKO mice displayed a significantly longer lifespan than WT concomitant with a higher ejection fraction and significantly slower heart rate. To test, whether the latter parameters depend on one another or were the result of a compensatory process, we reduced the heart rate pharmacologically (CCPA) and found that in mice, a slower heart rate is accompanied with a smaller not — as found for the dKO mice — increased ejection fraction (Fig. 2). At this point we would speculate that the longer lifespan of the dKO mice was a result of the slower heart rate (Fig. 4Ca). HRV analysis did not give evidence for a particular influence of $G\alpha_q/G\alpha_{11}$ signaling concerning the sympathetic or parasympathetic nervous system (see Fig. 4 in [20]). Despite such differences between the various genotypes, a study using working hearts ex vivo yielded no differences in ejection fraction. This was a surprising result because the increased ejection fraction in dKO mice in vivo was in agreement with increased Ca^{2+}-transients in ventricular myocytes isolated from dKO mice reported previously [14]. We can't provide a full explanation for the apparent discrepancy between cellular Ca^{2+}-transients and the working heart ejection fraction. However, to translate Ca^{2+}-signals into contraction requires further steps and hence offers the possibility of additional regulatory mechanisms such as the Ca^{2+}-sensitivity of the contractile filaments.

To address this puzzling finding we went back to the in vivo situation and measured the mean arterial pressure in the mice. We found that the mean arterial pressure was significantly reduced in a $G\alpha_{11}$-dependent manner. These findings strongly suggested that the increased ejection fraction found in the dKO mice measured in vivo might indeed be an off-target effect of $G\alpha_{11}$ KO rather than $G\alpha_q$-dependent. In contrast to the conditional $G\alpha_q$ KO, $G\alpha_{11}$-protein were absent globally. At this point we speculate that the reduced mean arterial

pressure was a result of $G\alpha_{11}$ KO in smooth muscle cells reducing the peripheral resistance. This hypothesis is supported by the following findings: (i) the ejection fraction of hearts from Gq-KO mice was not significantly different compared with WT hearts (see Fig. 2 in [20]); (ii) the global G11-KO mice exhibited a significantly higher ejection fraction than did the WT mice, as did the Gq-KO hearts (see Fig. 2 in [20]); and (iii) $G\alpha_q/G\alpha_{11}$ signaling in smooth muscle cells controls contractility and thus smooth muscle tone [30].

In recent reports, $G\alpha_q$-protein function was attributed to a reduced heart rate because of $G\alpha_q$-signaling specifically in the sinoatrial (SA) node the heart's primary pacemaker center [32]. In our study, we cannot directly support such findings, because the heart rate was not significantly different between Gq-KO and WT animals (Fig. 4Ca). Instead, G11-KO and the dKO of both G-proteins resulted in a significantly and maintained lower heart rate (Fig. 4Ca).

4.2. Remodeling of the extracellular matrix

Significantly increased fibrosis has been identified as a hallmark of cardiac hypertrophy [33] and hypertrophy was significantly reduced or absent in dKO mice as previously reported [8]. We thus addressed the putative role $G\alpha_q/G\alpha_{11}$-dependent signaling pathways may play for the production of the extracellular matrix in the heart. A longterm study on aging mice revealed that age-dependent increases in fibrosis were absent in Gq-KO and significantly reduced in G11-KO and dKO mice (Fig. 5). In a whole transcriptome Next Generation Sequencing study we identified that transcripts for collagens were upregulated. In contrast, transcripts coding for proteins responsible for the dynamic rearrangement and signaling of the extracellular matrix, the family of matricellular proteins [34] were substantially downregulated (Table 2). Our sequencing data demonstrated (Table 2) that the transcriptional activity of members of the CCN protein family [35] was substantially downregulated. A very prominent one was the cysteine-rich angiogenic inducer 61 (Cyr61) (Table 2, top line of lower portion). Cyr61 is reportedly involved in extracellular matrix production [36] and its expression has been shown to be regulated by the $G\alpha_q/G\alpha_{11}$ signaling pathway [35]. Therefore matricellular proteins might be the limiting factor for extracellular matrix formation independent of the expression level of other molecular constituents of the extracellular matrix.

Additionally, Cyr61 upregulation appears to accompany pressure-overload induced hypertrophy in a protein kinase C dependent manner [37] probably representing the link downstream to $G\alpha_q/G\alpha_{11}$ signaling [38]. It therefore appears likely that Gq-KO efficiently reduced or suppressed pressure-overload dependent hypertrophy because upregulation of matricellular gene activity is an important step resulting in an increased cardiac fibrosis that further fosters cardiac structural remodeling and cardiac malfunction.

5. Conclusions

Based on the in vivo characterization of Gq-KO, G11-KO and dKO mice we conclude that $G\alpha_{11}$ signaling in smooth muscle affects both cardiac afterload and cardiac performance and decreased heart rate in combination with decreased afterload appears to be the reason for the increased survival of the dKO mice compared with both the single-KOs and the WT mice. $G\alpha_{q/11}$ signaling diminishes age-dependent increases in fibrosis, most likely through down regulation of matricellular genes, presumably Cyr61 that regulates extracellular matrix formation and signaling.

Such the $G\alpha_q/G\alpha_{11}$ signaling and it's relation to cardiac hypertrophy is not related to single cell $G\alpha_q$ and $InsP_3$ signaling in ventricular myocytes, but a multiparametric systemic and organ based effect.

Supplementary data to this article can be found online at http://dx.doi.org/10.1016/j.ijcard.2015.10.069.

Conflict of interest

None of the authors declare potential conflicts of interest, including related consultancies, shareholdings and funding grants.

Acknowledgments

This research was funded by the Clinical Research Unit 196 (DFG [German Research Foundation]), and Saarland University (HOMFOR [Homburger Forschungsförderprogramm] and ZFK [Central Research Commission]). We would like to thank J. Kilper for assisting with the paraffin sectioning and S. Henning for the excellent cell isolation.

References

[1] D.G. Tilley, G protein-dependent and G protein-independent signaling pathways and their impact on cardiac function, Circ. Res. 109 (2011) 217–230.
[2] X. Li, A.V. Zima, F. Sheikh, L.A. Blatter, J. Chen, Endothelin-1-induced arrhythmogenic Ca^{2+} signaling is abolished in atrial myocytes of inositol-1,4,5-trisphosphate(IP3)-receptor type 2-deficient mice, Circ. Res. 96 (2005) 1274–1281.
[3] X. Wu, T. Zhang, J. Bossuyt, X. Li, T.A. McKinsey, J.R. Dedman, et al., Local InsP3-dependent perinuclear Ca^{2+} signaling in cardiac myocyte excitation–transcription coupling, 116 (2006) 675–682.
[4] H. Nakayama, I. Bodi, M. Maillet, J. DeSantiago, T.L. Domeier, K. Mikoshiba, et al., The IP3 receptor regulates cardiac hypertrophy in response to select stimuli, Circ. Res. 107 (2010) 659–666.
[5] D.D. D'Angelo, Y. Sakata, J.N. Lorenz, G.P. Boivin, R.A. Walsh, S.B. Liggett, et al., Transgenic Galphaq overexpression induces cardiac contractile failure in mice, Proc. Natl. Acad. Sci. U. S. A. 94 (1997) 8121–8126.
[6] S.A. Akhter, L.M. Luttrell, H.A. Rockman, G. Iaccarino, R.J. Lefkowitz, W.J. Koch, Targeting the receptor-Gq interface to inhibit in vivo pressure overload myocardial hypertrophy, Science 280 (1998) 574–577.
[7] J.H. Rogers, P. Tamirisa, A. Kovacs, C. Weinheimer, M. Courtois, K.J. Blumer, et al., RGS4 causes increased mortality and reduced cardiac hypertrophy in response to pressure overload, J. Clin. Invest. 104 (1999) 567–576.
[8] N. Wettschureck, H. Rütten, A. Zywietz, D. Gehring, T.M. Wilkie, J. Chen, et al., Absence of pressure overload induced myocardial hypertrophy after conditional inactivation of Galphaq/Galpha11 in cardiomyocytes, Nat. Med. 7 (2001) 1236–1240.
[9] L. Barki-Harrington, L.M. Luttrell, H.A. Rockman, Dual inhibition of beta-adrenergic and angiotensin II receptors by a single antagonist: a functional role for receptor–receptor interaction in vivo, Circulation 108 (2003) 1611–1618.
[10] D. Cervantes, C. Crosby, Y. Xiang, Arrestin orchestrates crosstalk between G protein-coupled receptors to modulate the spatiotemporal activation of ERK MAPK, Circ. Res. 106 (2010) 79–88.
[11] G.L. Christensen, S. Knudsen, M. Schneider, M. Aplin, S. Gammeltoft, S.P. Sheikh, et al., AT(1) receptor Gαq protein-independent signalling transcriptionally activates only a few genes directly, but robustly potentiates gene regulation from the β2-adrenergic receptor, Mol. Cell. Endocrinol. 331 (2011) 49–56.
[12] S. Offermanns, M.I. Simon, Genetic analysis of mammalian G-protein signalling, Oncogene 17 (1998) 1375–1381.
[13] M. Takefuji, A. Wirth, M. Lukasova, S. Takefuji, T. Boettger, T. Braun, et al., G(13)-mediated signaling pathway is required for pressure overload-induced cardiac remodeling and heart failure, Circulation 126 (2012) 1972–1982.
[14] S. Pahlavan, M. Oberhofer, B. Sauer, S. Ruppenthal, Q. Tian, A. Scholz, et al., Gαq and Gα11 contribute to the maintenance of cellular electrophysiology and Ca^{2+} handling in ventricular cardiomyocytes, Cardiovasc. Res. 95 (2012) 48–58.
[15] L. Kaestner, A. Scholz, K. Hammer, A. Vecerdea, S. Ruppenthal, P. Lipp, Isolation and genetic manipulation of adult cardiac myocytes for confocal imaging, J. Vis. Exp. 31 (2009).
[16] J.E. Camacho Londoño, Q. Tian, K. Hammer, L. Schröder, J. Camacho Londoño, J.C. Reil, et al., A background Ca^{2+} entry pathway mediated by TRPC1/TRPC4 is critical for development of pathological cardiac remodelling, Eur. Heart J. 36 (2015) 2257–2266.
[17] K. Hammer, S. Ruppenthal, C. Viero, A. Scholz, L. Edelmann, L. Kaestner, et al., Remodelling of Ca^{2+} handling organelles in adult rat ventricular myocytes during long term culture, J. Mol. Cell. Cardiol. 49 (2010) 427–437.
[18] M. Oberhofer, Q. Tian, S. Ruppenthal, S. Wegener, J.-C. Reil, C. Körbel, et al., Calcium dysregulation in ventricular myocytes from mice expressing constitutively active Rac1, Cell Calcium 54 (2013) 26–36.
[19] J. Thireau, B.L. Zhang, D. Poisson, D. Babuty, Heart rate variability in mice: a theoretical and practical guide, Exp. Physiol. 93 (2007) 83–94.
[20] K. Wiesen, E. Kaiser, L. Schröder, S. Ruppenthal, J.-C. Reil, P. Lipp, Supporting evidence for Cardiac remodeling in $G\alpha_q$ and $G\alpha_{11}$ knockout mice, Data in Brief (2007)http://dx.doi.org/10.1016/j.ijcard.2015.10.069.
[21] J.C. Reil, M. Hohl, M. Oberhofer, A. Kazakov, L. Kaestner, P. Mueller, et al., Cardiac Rac1 overexpression in mice creates a substrate for atrial arrhythmias characterized by structural remodelling, Cardiovasc. Res. 87 (2010) 485–493.
[22] D. Kim, G. Pertea, C. Trapnell, H. Pimentel, R. Kelley, S.L. Salzberg, TopHat2: accurate alignment of transcriptomes in the presence of insertions, deletions and gene fusions, Genome Biol. 14 (2013) R36.

[23] C. Trapnell, B.A. Williams, G. Pertea, A. Mortazavi, G. Kwan, M.J. van Baren, et al., Transcript assembly and quantification by RNA-Seq reveals unannotated transcripts and isoform switching during cell differentiation, Nat. Biotechnol. 28 (2010) 511–515.
[24] C. Trapnell, A. Roberts, L. Goff, G. Pertea, D. Kim, D.R. Kelley, et al., Differential gene and transcript expression analysis of RNA-seq experiments with TopHat and Cufflinks, Nat. Protoc. 7 (2012) 562–578.
[25] C. Backes, A. Keller, J. Kuentzer, B. Kneissl, N. Comtesse, Y.A. Elnakady, et al., GeneTrail—advanced gene set enrichment analysis, Nucleic Acids Res. 35 (2007) W186–W192.
[26] M. Kanehisa, S. Goto, KEGG: kyoto encyclopedia of genes and genomes, Nucleic Acids Res. 28 (2000) 27–30.
[27] M.A. Harris, J. Clark, A. Ireland, J. Lomax, M. Ashburner, R. Foulger, et al., The Gene Ontology (GO) database and informatics resource, Nucleic Acids Res. 32 (2004) D258–D261.
[28] M.D. Muzumdar, B. Tasic, K. Miyamichi, L. Li, L. Luo, A global double-fluorescent Cre reporter mouse, Genesis 45 (2007) 593–605.
[29] A. Conti, A. Monopoli, M. Gamba, P.A. Borea, E. Ongini, Effects of selective A1 and A2 adenosine receptor agonists on cardiovascular tissues, Naunyn Schmiedeberg's Arch. Pharmacol. 348 (1993) 108–112.
[30] J.J. Maguire, A.P. Davenport, Regulation of vascular reactivity by established and emerging GPCRs, Trends Pharmacol. Sci. 26 (2005) 448–454.
[31] D.F. Mosher, J.C. Adams, Adhesion-modulating/matricellular ECM protein families: a structural, functional and evolutionary appraisal, Matrix Biol. 31 (2012) 155–161.
[32] E. Kaiser, Q. Tian, M. Barth, S. Ruppenthal, J. Wess, L. Kaestner, et al., Gq signaling in the heart impacts primary pacemaking and conduction propagation, Acta Physiol. 213 (2015) 117.
[33] K.T. Weber, C.G. Brilla, S.E. Campbell, Regulatory mechanisms of myocardial hypertrophy and fibrosis: results of in vivo studies, Cardiology 81 (1992) 266–273.
[34] P. Bornstein, Matricellular proteins: an overview, J. Cell Commun. Signal 3 (2009) 163–165.
[35] C.T. Walsh, D. Stupack, J.H. Brown, G protein-coupled receptors go extracellular: RhoA integrates the integrins, Mol. Interv. 8 (2008) 165–173.
[36] Y. Chen, X.-Y. Du, Functional properties and intracellular signaling of CCN1/Cyr61, J. Cell. Biochem. 100 (2007) 1337–1345.
[37] D. Hilfiker-Kleiner, K. Kaminski, A. Kaminska, M. Fuchs, G. Klein, E. Podewski, et al., Regulation of proangiogenic factor CCN1 in cardiac muscle: impact of ischemia, pressure overload, and neurohumoral activation, Circulation 109 (2004) 2227–2233.
[38] X. Hui, G. Reither, L. Kaestner, P. Lipp, Targeted activation of conventional and novel protein kinase C through differential translocation patterns, Mol. Cell. Biol. 24 (2014) 2370–2381.

Danksagung

Hiermit möchte ich allen danken, die an dem Zustandekommen dieser Arbeit beteiligt waren.

Mein ganz besonderer Dank geht an meinen Betreuer PD Dr. Lars Kästner und an Prof. Dr. Peter Lipp, denen bis zum Schluss keine Erläuterung auch noch so komplexer Fragestellungen zu viel gewesen ist. Die mir sowohl während der Datenauswertung, als auch beim späteren Niederschreiben der Studienergebnisse immer und jederzeit mit Rat und Tat zur Seite gestanden haben.

Ein weiterer besonderer Dank gilt meiner Doktormutter PD Dr. Anna Bogdanova, die mir immer so schnell und so gut es ihr möglich war zur Seite stand und mich im Voranschreiten meiner Arbeit immer bestmöglich unterstützte.

Auch meinen beiden Nachfolgerinnen im Institut für Molekulare Zellbiologie, Elisabeth Kaiser und Laura Schröder, möchte ich von ganzem Herzen für ihre Unterstützung und aufbauenden Worte vor allem in harten Zeiten danken.

Insbesondere möchte ich meinen Eltern, vor allem meinem Papa, danken, denen diese Doktorarbeit gewidmet ist. Sie haben mir die Universitätsausbildung ermöglicht, mir jederzeit in jeglicher Hinsicht zur Seite gestanden und mich nicht nur während des Studiums immer wieder aufgebaut, und auch bis zuletzt fortlaufend ermuntert und bestärkt, die vorliegende Arbeit fertigzustellen.

Ein weiterer tiefer Dank geht an meine beiden tierischen Begleiter Pandora und Paula, die mich auch in schweren Zeiten immer wieder aufgefangen haben.

Auch meine Geschwister Laura, David und Joshua und mein Lebensgefährte Holger haben meine Höhen und Tiefen mitgetragen und waren immer für mich da, wenn ich sie brauchte.

Kathrina Wiesen

Curriculum Vitae tabellarisch

Vorname Name	Kathrina Wiesen
Geburtsdatum	15/01/1982
Geburtsort	Quierschied, Deutschland
Nationalität	Deutsch

Schulausbildung (Schulbezeichnung, Ort Land)

08/1988 - 07/1992	Grundschule, Uchtelfangen, Deutschland
08/1992 - 06/2001	Illtal Gymnasium, Illingen, Deutschland

Höchster Schulabschluss (Abitur, Schule, Ort, Land)

08.06.2001	Abitur, Illtal Gymnasium, Illingen, Deutschland

Studium

09/2001- 03/2007	Veterinärmedizin, Justus Liebig Universität, Gießen, Deutschland
19.02.2007	Abschlussprüfung vet.med. Staatsexamen, Justus Liebig Universität, Gießen, Deutschland
02/2012 - 10/2015	Anfertigung der Dissertation unter Leitung von PD Dr. Anna Bogdanova, Institut für Veterinärphysiologie, Vetsuisse-Fakultät Universität Zürich, Schweiz

Alle fachrelevanten Anstellungen nach Abschluss des veterinärmedizinischen Studiums

06/2007 - 06/2009	Assistenztierärztin Kleintierpraxis Majka Kiefer, Altforweiler, Deutschland
07/2009 - 12/2012	Wissenschaftliche Mitarbeiterin, Universitätskliniken des Saarlandes, Institut für Zellbiologie, Homburg/Saar, Deutschland
01-2013 - 09/2014	Senior Scientist DSM (Drug Safety and Metabolism), MSD Animal Health, Preclinical Development, Schwabenheim, Deutschland
10/2014 - 03/2015	Assistenztierärztin Tierarztpraxis Markus Doebbeler, Völklingen, Deutschland